© 2021. Published by The Company of Biologists Ltd | Development (2021) 148, dev199414. doi:10.1242/dev.199414

RESEARCH ARTICLE

Mouse EWSR1 is crucial for spermatid post-meiotic transcription and spermiogenesis

Hui Tian and Petko M. Petkov*

ABSTRACT

Spermatogenesis is precisely controlled by complex gene-expression programs. During mammalian male germ-cell development, a crucial feature is the repression of transcription before spermatid elongation. Previously, we discovered that the RNA-binding protein EWSR1 plays an important role in meiotic recombination in mouse, and showed that EWSR1 is highly expressed in late meiotic cells and post-meiotic cells. Here, we used an *Ewsr1* pachytene stage-specific knockout mouse model to study the roles of *Ewsr1* in late meiotic prophase I and in spermatozoa maturation. We show that loss of EWSR1 in late meiotic prophase I does not affect proper meiosis completion, but does result in defective spermatid elongation and chromocenter formation in the developing germ cells. As a result, male mice lacking EWSR1 after pachynema are sterile. We found that, in *Ewsr1* CKO round spermatids, transition from a meiotic gene-expression program to a post-meiotic and spermatid gene expression program related to DNA condensation is impaired, suggesting that EWSR1 plays an important role in regulation of spermiogenesis-related mRNA synthesis necessary for spermatid differentiation into mature sperm.

KEY WORDS: Meiosis, EWSR1, Spermiogenesis

INTRODUCTION

Reproductive failure affects 10-15% of couples worldwide, up to 55% of which is due to spermatogenic failure (Visser and Repping, 2010). Spermatogenesis is a tightly regulated process during which germ cells originating from spermatogonial stem cells progress through several developmental stages and ultimately produce highly differentiated spermatozoa. During this development, spermatogonial stem cells enter the proliferation cycle as spermatogonia, which in turn differentiate into spermatocytes that undergo meiosis and produce haploid round spermatids. The round spermatids in mammals then go through complex biochemical and morphological changes, and further develop into elongated spermatids and eventually into mature sperm cells. This dramatic post-meiotic differentiation process, termed spermiogenesis, includes acrosome and flagellum formation, nuclear condensation and cytoplasmic exclusion (Hess and Renato de Franca, 2008). A crucial feature of spermiogenesis is the repression of transcription before spermatid elongation. Thus, mRNAs required for post-meiotic spermatid differentiation are synthesized in spermatocytes and round spermatids, but then become translationally repressed and stored. As spermiogenesis progresses, those mRNAs are gradually released and spermatid differentiation-relevant proteins are synthesized (Steger, 1999). Regulation of the transcriptional repression and translational inactivation during spermatid development involves multiple factors and pathways, including non-coding RNAs (de Mateo and Sassone-Corsi, 2014; Meikar et al., 2011), replacement of histones by protamines (Barral et al., 2017; Rathke et al., 2014), RNA alternative splicing (Margolin et al., 2014; Schmid et al., 2013), transcription-factor and RNA-binding protein activation (Idler and Yan, 2012; Paronetto and Sette, 2010), and functions of RNA processing granules (de Mateo and Sassone-Corsi, 2014; Meikar et al., 2011). However, the mechanisms of action and the functions of these factors and pathways are not fully characterized.

Ewing sarcoma RNA-binding protein 1 (EWSR1) is a member of the TET family (TLS/FUS, EWS and TAF-II68) RNA- and DNA-binding proteins (Tan and Manley, 2009). In many somatic cell types, these proteins play important functions in transcription, RNA processing and tumorigenesis. The C-terminal regions of TET proteins contain several RNA-binding motifs, including three arginine-glycine-glycine (RGG) boxes, one RNA recognition motif (RRM) and one zinc-finger domain (Schwartz et al., 2015). The N-terminal domains of these proteins are rich in glutamine, serine and tyrosine; are capable of activating transcription; and are frequently involved in tumor-derived fusions with other genes (Delattre et al., 1992; Schwartz et al., 2015). In addition, EWSR1 interacts with multiple RNA-binding proteins and plays a role in various nuclear processes. For example, it is involved in transcriptional regulation via binding to the preinitiation complex TFIID and with subunits of RNA polymerase II (RNA POLII) (Bertolotti et al., 1998; Petermann et al., 1998; Yang et al., 2000); it influences microRNA (miRNA) activity by regulating expression of the miRNA processing protein Drosha (Kim et al., 2014); it interacts with several RNA alternative splicing factors, such as TASR1/2 (Yang et al., 2000), U1C (Knoop and Baker, 2000) and YB1 (Chansky et al., 2001); and it regulates DNA damage-induced RNA splicing (Paronetto et al., 2011).

We have reported that, during spermatogenesis, EWSR1 is one of the key regulators of meiotic recombination, by interacting with recombination hotspot determinator PRDM9 and meiotic-specific cohesin REC8 in leptotene and zygotene spermatocytes (Parvanov et al., 2017; Tian et al., 2021). Furthermore, although neither we nor others detected a function of EWSR1 in regulating gene expression or RNA binding during these prophase I stages, some of our findings indicated that EWSR1 may be involved in post-meiotic differentiation. Specifically, we showed that EWSR1 expression increased dramatically in pachytene and diplotene spermatocytes, and round spermatids in mouse testes (Parvanov et al., 2017). This prompted us to elucidate the function of EWSR1 in spermiogenesis.

To achieve this goal, we created an *Ewsr1* pachytene stage-specific knockout mouse model, allowing us to separate its functions during late meiotic prophase I and spermatozoa maturation from those

The Jackson Laboratory, Bar Harbor, ME 04609, USA.

*Author for correspondence (petko.petkov@jax.org)

P.M.P., 0000-0002-6694-9150

Handling Editor: Swathi Arur
Received 7 January 2021; Accepted 18 May 2021

Development (2021) 148, dev199414. doi:10.1242/dev.199414

in early meiosis that we have already described (Tian et al., 2021). We now show that loss of EWSR1 at this stage does not affect proper meiosis completion, but that developing germ cells exhibit defects in spermatid elongation and chromocenter formation. In *Ewsr1* conditional knockout testes, expression of many genes regulating spermatid differentiation is impaired, suggesting that EWSR1 plays an important role in regulation of spermiogenesis-related mRNA synthesis, thereby enabling spermatid differentiation into mature sperm.

RESULTS

Late meiotic stage-specific inactivation of *Ewsr1* results in the absence of spermatozoa and in male infertility

In a previous study, we showed that, in juvenile mouse testes, EWSR1 is expressed highly in both spermatogonia and Sertoli cells, and at lower levels in early spermatocytes (Parvanov et al., 2017). In the present study, we show that, in adult mouse testes, EWSR1 expression is high in spermatogonia and then decreases at the pre-leptotene stage, when STRA8, a spermatocyte development-regulating protein, is expressed (Fig. 1A, far right panel, stage VII-VIII). The EWSR1 signal remains relatively low in leptotene/zygotene spermatocytes, and then dramatically increases at pachynema and remains high in diplotene spermatocytes and round spermatids, eventually disappearing from elongated spermatids (stage X) (Parvanov et al., 2017; Tian et al., 2021). The EWSR1 signal is absent in heterochromatin regions, which are labeled by H3K9me3 (histone-3 trimethylated at lysine 9), such as the sex body at pachynema, as previously shown (Parvanov et al., 2017; Tian et al., 2021), or the chromocenter in round spermatids, as we show here (Fig. 1B). From this overall expression pattern, we speculated that EWSR1 may play a role in post-meiotic differentiation.

To determine the function of EWSR1 in late meiotic and post-meiotic stages, we used a conditional knockout approach to delete *Ewsr1* from spermatocytes using *Hspa2* promoter-driven CRE ($Ewsr1^{loxp/\Delta;Hspa2\text{-}Cre}$; hereafter referred to as *Ewsr1* CKO). *Hspa2-Cre* mice express CRE from zygonema onward (Inselman et al., 2010). We did not detect any adverse health effects due to potential *Hspa2-Cre* expression in other tissues. In the CKO testes, EWSR1 protein levels were lower than in testes of heterozygous controls ($Ewsr1^{loxp/+;Hspa2\text{-}Cre}$; hereafter referred to as *Ewsr1* het) (Fig. 2A). Immunostaining of CKO seminiferous tubules showed that the EWSR1 signal in zygotene spermatocytes in stage XI seminiferous tubules was comparable in strength with that in the heterozygous control (Fig. 2B, left-hand panels, white arrows), but completely disappeared at pachynema and in round spermatids (Fig. 2B, right-hand panels, arrowheads). The EWSR1 signal in Sertoli cells was not affected (Fig. 2B, right-hand panels, arrows). These results indicate that EWSR1 expression is indeed abolished from the pachytene stage onward in *Ewsr1* CKO testes.

Loss of *Ewsr1* from pachytene spermatocytes led to a slight but significant reduction of testis size compared with heterozygous control testes in adult mice (Fig. 2C, $P<0.05$). *Ewsr1* CKO mice were sterile. No offspring were produced by *Ewsr1* CKO male mice when mated to C57BL/6J females, while control matings of *Ewsr1* het male mice produced normal numbers of viable pups (7.0±3.0 pups per litter, Fig. 2D). Histological examination showed that *Ewsr1*-deficient seminiferous tubules lost spermatids, whereas the morphology of Sertoli cells, spermatogonia and spermatocytes was preserved (Fig. 2E). In addition, stage VII-VIII spermatid arrest in *Ewsr1*-deficient seminiferous tubules was confirmed by co-staining of EWSR1 and STRA8 on CKO testicular cross-sections (Fig. S1A). Furthermore, multinucleated cells with pyknotic nuclei were observed in CKO seminiferous tubules (Fig. 2E, arrows), suggesting both germ-cell apoptosis (Nantel et al., 1996) and seminiferous-tubule atrophy in *Ewsr1*-deficient testes.

During spermiogenesis, spermatid elongation begins in step 8 spermatids, in which microtubules are assembled to form a semi-circular (skirt-like) band structure, termed a manchette, around the caudal pole of elongated spermatid nuclei (Fig. S1B, left panel). β-Tubulin, one of the proteins participating in manchette assembly (Fujii et al., 2017; Lehti and Sironen, 2016), can be used as a marker of spermatid elongation. In CKO tubules, a skirt-like manchette structure was not observed (Fig. S1B, right panel), further indicating that no elongated spermatids were present in CKO testes. In additional, no spermatozoa were observed in the *Ewsr1* CKO epididymis, whereas they were plentiful in the het control (Fig. 2E, lower panels). Together, these results suggest that the absence of spermatozoa in in testes lacking EWRS1 expression from the pachytene stage onward is likely the result of a block of spermatid differentiation.

Loss of EWSR1 in pachytene spermatocytes does not affect meiotic progression

During meiosis, EWSR1 plays a role in meiotic recombination initiation and determination by interacting with PRDM9 and

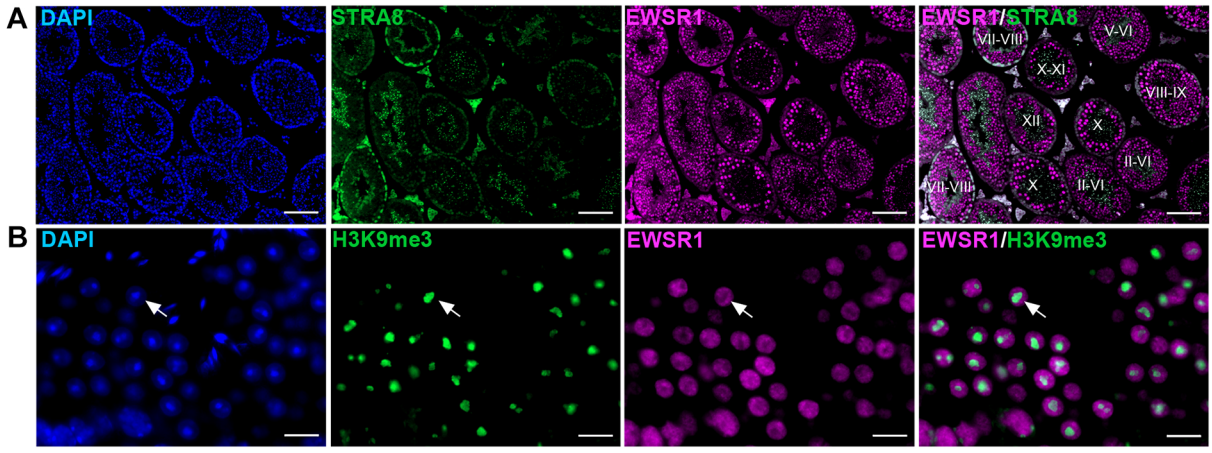

Fig. 1. EWSR1 is highly expressed in euchromatin regions of late spermatocytes and round spermatids. (A) Co-staining of EWSR1 (magenta) and STRA8 (green) on adult B6 testicular sections. Scale bars: 100 µm. The Roman numerals indicate the stage of each seminiferous tubule. (B) Co-staining of EWSR1 (magenta) and the heterochromatin marker H3K9me3 (green). White arrows indicate round spermatids. Scale bars: 10 µm.

Development (2021) 148, dev199414. doi:10.1242/dev.199414

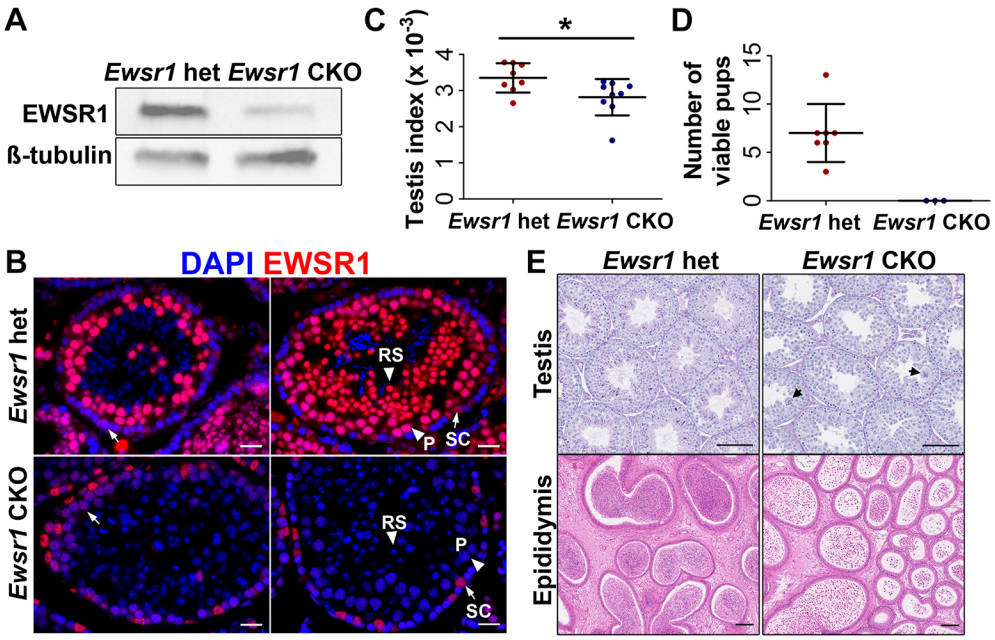

Fig. 2. *Ewsr1* CKO mice are sterile with post-meiotic arrest. (A) Western blotting confirmed reduced EWSR1 protein levels in the *Ewsr1* CKO testis. (B) Immunostaining of EWSR1 (red) in *Ewsr1* het (top panels) and CKO (bottom panels) testes. Arrows in the left-hand panels indicate leptonema; arrows in the right-hand panels indicate Sertoli cells (SCs); arrowheads in the right-hand panels indicate pachynema (P) and round spermatids (RSs). Scale bars: 20 µm. (C) Testis index (testis weight/body weight) in *Ewsr1* het and CKO mice. **P*<0.05 by Student's *t*-test. (D) Fertility test in *Ewsr1* het (*n*=3) and CKO (*n*=3) male mice. (E) PAS staining of seminiferous tubule sections (top panels), and Hematoxylin and Eosin staining of epididymis sections (bottom panels) in *Ewsr1* het (left) and CKO (right) mice. Arrows indicate multinucleated cells with pyknotic nuclei in *Ewsr1* CKO seminiferous tubules. Scale bars: 50 µm. Data are mean±s.d.

pREC8, a chromosome axis protein, and stabilizing the PRDM9-hotspot DNA/chromosomal axis complex at the leptotene and zygotene stages (Tian et al., 2021). Knocking out *Ewsr1* in mice, either systemically or conditionally at the onset of meiosis, leads to meiotic prophase I arrest with increased chromosomal asynapsis (Li et al., 2007; Tian et al., 2021). To investigate whether loss of EWSR1 from pachytene cells also affects meiotic progression, we first examined DNA double-strand break (DSB) formation and repair using phosphorylated H2AX (γH2AX, a marker for unrepaired DNA lesions) staining on *Ewsr1* CKO and het spermatocyte chromosome spreads. CKO spermatocytes showed no increase in the level of unrepaired DSBs or asynapsis (98.9% fully synapsed pachynema) relative to het controls (97.8% fully synapsed pachynema) (Fig. 3A and Fig. S2), while about 30% of systemic *Ewsr1* knockout spermatocytes showed chromosome asynapsis (Li et al., 2007). Next, we used ATR and HORMAD1 staining as markers for unsynapsed chromosomes, to examine the effect of EWSR1 loss on sex body formation and chromosomal synapsis. In both control and CKO pachytene spermatocytes, round-spread ATR signal covers only the sex chromosomes (Fig. 3B), and HORMAD1 is retained only on the sex chromosomes (Fig. 3C). Together, these data indicate that chromosomal synapsis and DSB formation are not impaired in *Ewsr1* CKO testes.

Systemic knockout of *Ewsr1* leads to remarkably reduced numbers of crossovers and increased numbers of bivalents without crossovers (Li et al., 2007; Tian et al., 2021). However, loss of EWSR1 from the pachytene stage onward showed no impact on crossover number (24.0±2.0 MLH1 foci per pachytene cell, *n*=70, from two individual mice; Fig. 3D,E) relative to het controls (23.7±2.0 MLH1 foci per pachytene cell, *n*=63, from two individual mice). Chiasma formation in the diplotene stage in *Ewsr1* CKO testes was also normal (Fig. S2). *Stra8-iCre*-mediated *Ewsr1* CKO

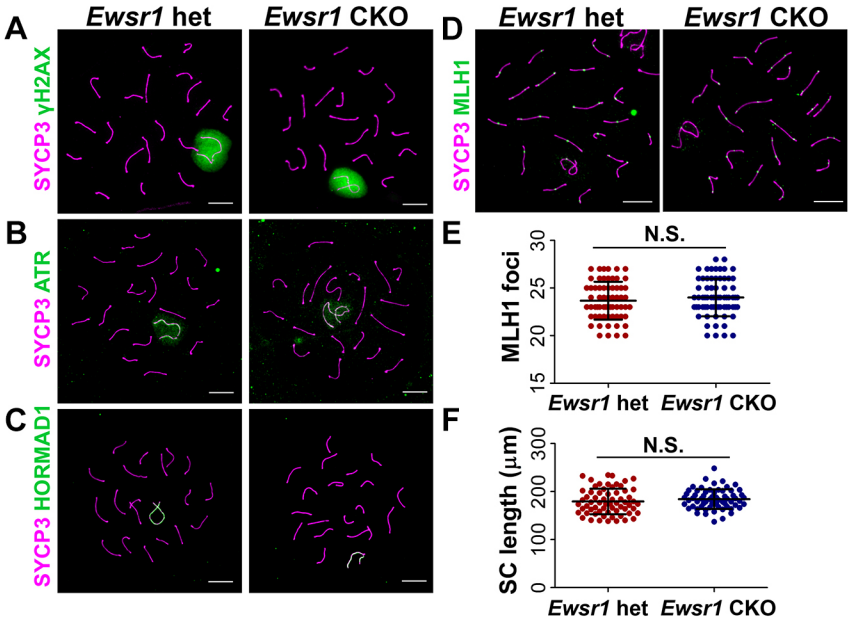

Fig. 3. Meiotic recombination is not affected in the *Ewsr1* CKO testis. (A-D) Co-immunostaining of SYCP3 (magenta) and γH2AX (A), ATR (B), HORMAD1 (C) or MLH1 (D) (green) in *Ewsr1* het and CKO mice. Scale bars: 10 µm. (E) MLH1 foci number in *Ewsr1* het (*n*=63 from two individual mice) and CKO (*n*=70 from two individual mice) pachynema spermatocytes. (F) Synaptonemal complex length measured by SCYP3 in *Ewsr1* het (*n*=65 from two individual mice) and CKO (*n*=64 from two individual mice) pachynema spermatocytes. N.S., not significant (*P*>0.05 by Student's *t*-test). Data are mean±s.d.

Development (2021) 148, dev199414. doi:10.1242/dev.199414

spermatocytes showed both insufficient numbers of crossovers and shorter synaptonemal complex (SC) length at the pachytene stage (Tian et al., 2021). However, in *Hspa2-Cre*-mediated *Ewsr1* CKO spermatocytes, SC length (184.1±20.5 µm, *n*=64, from two individuals; Fig. 3F) was similar to that in heterozygous controls (179.3±26.6 µm for total SC length, *n*=65, from two individuals), consistent with the results for crossover numbers in *Hspa2-Cre*-mediated *Ewsr1* CKO testes. Together, these results suggest that loss of EWSR1 from the pachytene stage onward does not affect crossover determination.

Overall, these results suggest that loss of *Ewsr1* from the pachytene stage onward does not cause any meiotic defects. It demonstrates that during spermatid differentiation and spermiogenesis, EWSR1 has a post-meiotic function that is independent of its function in meiotic recombination.

Chromocenter formation is impaired in *Ewsr1* CKO spermatids

Nuclear topology is reorganized during spermiogenesis (Brinkley et al., 1986), when the centromeric heterochromatin domains form one or two chromocenters in round and elongated spermatids (Berkovits and Wolgemuth, 2013; Hoyer-Fender et al., 2000; Namekawa et al., 2006). To investigate whether EWSR1 functions in chromocenter formation, we carried out immunostaining with antibodies against H3K9me3 to label chromocenters and against CREST to label centromeres. In *Ewsr1* het round spermatids, chromocenter formation was normal; centromeres coalesced and colocalized with the H3K9me3 signal to form a single focus (Fig. 4A, top panels), and only ∼8.4% of het round spermatids showed more than two chromocenters per cell (*n*=1097 spermatids, Fig. 4B). However, we observed chromocenter fragmentation in *Ewsr1* CKO round spermatids, most of which contained three or more H3K9me3/CREST foci (Fig. 4A, lower panels). The proportion of round spermatids with fragmented chromocenters was significantly increased (∼84.5%) in *Ewsr1* CKO spermatids. (*n*=1031 spermatids; Fig. 4B, *P*<0.001) To further confirm these results, we performed the same staining on *Ewsr1* CKO and het haploid round spermatids isolated by flow cytometry (Fig. S3), and observed the same chromocenter fragmentation phenotype in *Ewsr1* CKO spermatids (Fig. S4). These data indicate that absence of EWSR1 from the pachytene stage onward leads to abnormal chromatin condensation during spermatid differentiation.

Spermiogenesis-associated gene-expression profile is altered in *Ewsr1* CKO mice

To investigate whether spermiogenesis defects in the *Ewsr1* CKO mice are a consequence of altered gene expression, we performed RNA-seq in flow cytometry-sorted diploid cells, which contain primarily pachytene and diplotene spermatocytes (4c DNA content, hereafter referred to as P/D spermatocytes), and haploid cells, which represent round spermatids (1c DNA content, hereafter referred to as RS) (Figs S3 and S5A).

In P/D cells, 558 genes were differentially expressed between *Ewsr1* CKO and het control mice (*P*<0.05, Wilcoxon rank sum test). Of these, 408 were upregulated and 150 were downregulated in CKO mice (Fig. 5A, green dots, upregulated; yellow dots, downregulated). In RS, 937 genes were differentially expressed between *Ewsr1* CKO and het RS. Of these, 794 were upregulated and 143 were downregulated in CKO RS (Fig. 5A). Gene ontology analysis indicated enrichment of meiotic cell cycle-related genes (GO:0051321) in the group of genes upregulated in the CKO RS (FDR=1.14×10^{-2}).

The upregulation of meiosis-related genes in CKO RS suggested that the meiotic cell cycle was altered in these cells. To test whether this could be the case, we first compared the P/D het and RS het RNA-seq datasets, and identified 2577 genes that showed higher expression in P/D cells than in RS(p_{adj} <0.05, Wilcoxon rank sum test; Fig. S5B left, columns 1 and 3). We termed these genes P/D-enriched genes. Conversely, 1476 genes showed significantly higher expression in RS compared with P/D cells (p_{adj} <0.05, Wilcoxon rank sum test; Fig. S5B right, columns 1 and 3). We termed these genes RS-enriched genes.

Next, we compared the expression of P/D-enriched genes between *Ewsr1* CKO P/D cells and het P/D cells, and between CKO RS and het RS; and expression of RS-enriched genes between *Ewsr1* CKO P/D cells and het P/D cells, and between *Ewsr1* CKO RS and het RS. We found that expression of P/D-enriched genes was not significantly affected in CKO P/D cells (p_{adj}=0.042, Wilcoxon rank sum test; Fig. 5B left, red dots; Fig. 5C left, columns 1 and 2). However, these genes retained higher expression levels in CKO RS than in het controls ($p_{adj}=2.2\times10^{-12}$, Wilcoxon rank sum test; Fig. 5B right, red dots; Fig. 5C left, columns 3 and 4). We tested these overall results for expression of P/D-enriched genes, using qRT-PCR, and identified four meiosis-specific genes that showed no differential expression between P/D CKO cells and P/D het cells, and that also showed higher expression levels in *Ewsr1* CKO RS than in het RS (Fig. 5D). Of these four genes, *Cntd1* and *Mlh1* are crucial for normal meiotic crossover formation (Holloway et al., 2014; Santucci-Darmanin et al., 2000); *Mov10l1*, a gene involved in piRNA biogenesis, is predominantly expressed in pachytene spermatocytes, and its mRNA normally disappears in post-meiotic cells (Frost et al., 2010; Vourekas et al., 2015); and *Sycp3* codes for a component of the synaptonemal complex, and is expressed only in spermatocytes during spermatogenesis.

In contrast to these results for PD-enriched genes, most of the RS-enriched genes were downregulated in *Ewsr1* CKO RS compared with het RS (p_{adj}=0.006, Wilcoxon rank sum test; Fig. 5B right, blue dots; Fig. 5C right, columns 3 and 4). The expression of these

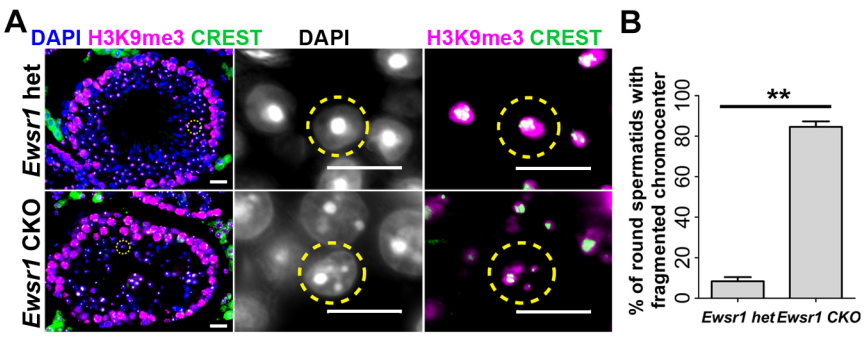

Fig. 4. Increased chromocenter fragmentation is observed in the absence of EWSR1. (A) Co-immunostaining of H3K9me3 (magenta) and centromeres (CREST, green) in *Ewsr1* het (top panels) and CKO (bottom panels) spermatids. Scale bars: 20 µm (left-hand panels); 10 µm (right-hand panels). (B) Percentage of round spermatids with fragmented chromocenters in *Ewsr1* het (*n*=1031 spermatids from two individual mice) and CKO (*n*=1097 spermatids from two individual mice) testes. ***P*<0.01 by Student's *t*-test. Data are mean±s.d.

Development (2021) 148, dev199414. doi:10.1242/dev.199414

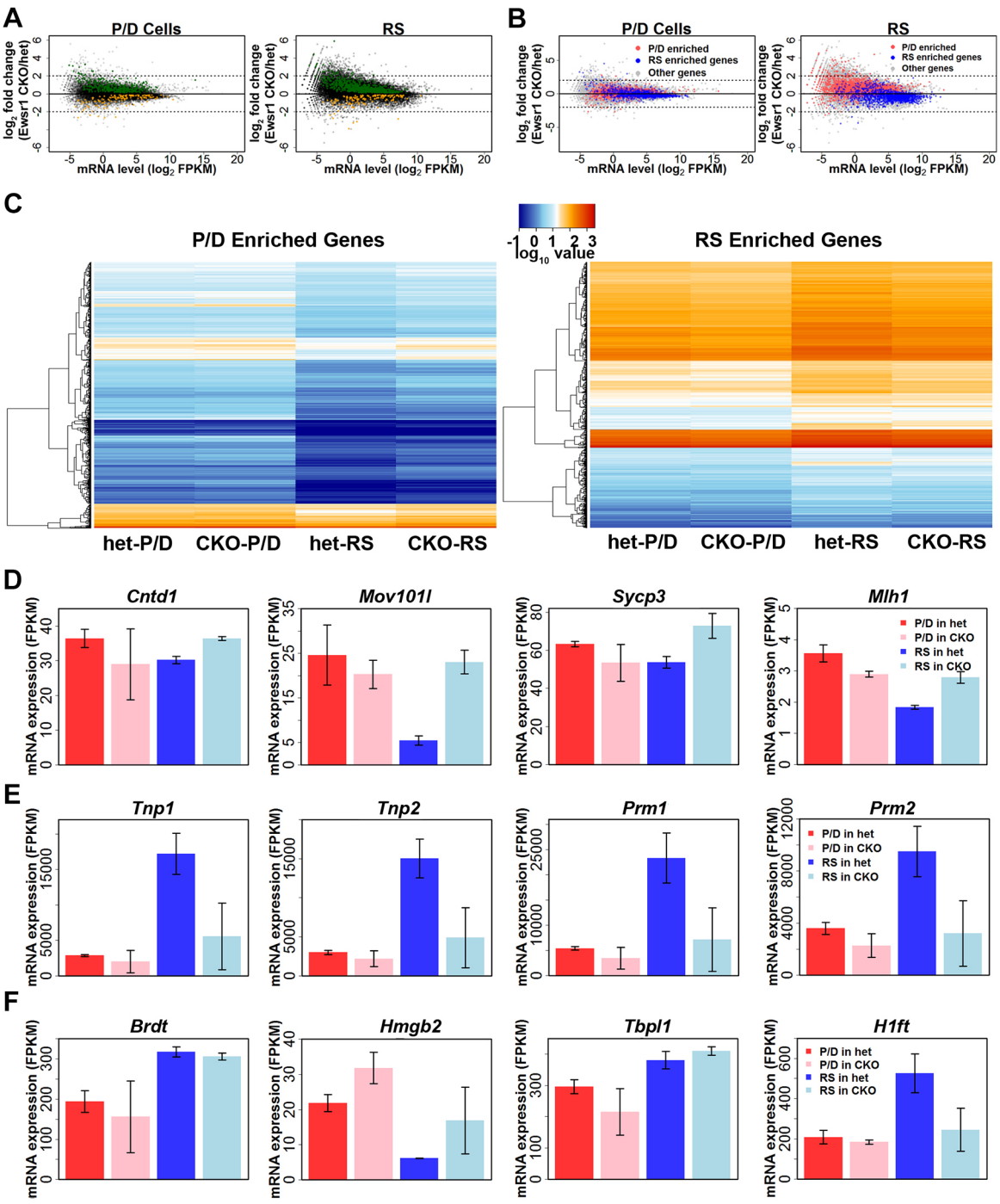

Fig. 5. RNA-seq of isolated spermatocytes and round spermatids in *Ewsr1* het and CKO mice. (A) MA plot of differentially expressed genes in pachynema/diplonema (P/D, left panel) and round spermatids (RS, right panel). *Y*-axis represents the $\log_2$ FPKM ratio of *Ewsr1* CKO versus het; *x*-axis represents the total $\log_2$ FPKM level of each gene. Green dots indicate genes significantly upregulated in CKO mice; yellow dots indicate genes significantly downregulated in CKO mice. (B) Distribution of P/D- or RS-enriched genes in P/D cells (left panel) and RS (right panel). *Y*-axis represents the $\log_2$ FPKM ratio of *Ewsr1* CKO versus het; *x*-axis represents the total $\log_2$ FPKM level of each gene. Red dots indicate P/D-enriched genes; blue dots indicate RS-enriched genes. (C) Heat map of P/D- and RS-enriched genes (left and right panels, respectively) in het P/D, CKO P/D, het RS and CKO RS samples. Key is shown between the two panels. (D-F) Confirmation of gene expression by qPCR in het P/D cells (red), CKO P/D cells (pink), het RS (dark blue) and CKO RS (light blue). (D) Meiosis-specific genes. (E) RS-enriched genes. (F) Chromocenter-related genes. Data are mean±s.d.

genes in CKO P/D cells showed no major differences in comparison with expression in het P/D controls (p_{adj}=0.16, Wilcoxon rank sum test; Fig. 5B left, blue dots; Fig. 5C right, columns 1 and 2). Genes downregulated in CKO RS compared with het RS controls included genes required for normal spermatid elongation, DNA packaging and chromatin condensation, including genes coding for protamines (*Prm1* and *Prm2*) (Cho et al., 2001), and transition nuclear proteins (*Tnp1* and *Tnp2*) (Shirley et al., 2004) (Fig. 5E). This misregulation could explain the cell-cycle arrest and DNA-packaging and -condensation defects that we observed in CKO spermatids.

Development (2021) 148, dev199414. doi:10.1242/dev.199414

Because we observed disruption of chromocenter formation, we also analyzed the expression of genes known to have functions related to RS chromocenter formation: *H1fnt* (*H1f7*), *Brdt*, *Hmgb2* and *Tbpl1*. *H1fnt* codes for a histone H1-like, haploid germ cell-specific nuclear protein that is required for DNA condensation and chromocenter formation in spermatids (Martianov et al., 2005; Tanaka et al., 2005); *Brdt* codes for a testis-specific double bromodomain protein that is required for chromocenter organization, depending on the genetic background (Berkovits and Wolgemuth, 2011); *Hmgb2* codes for a protein that is crucial for chromocenter and acrosome formation in spermatids (Catena et al., 2006; Ronfani et al., 2001); and *Tbpl1* is required for chromocenter formation and maintenance (Catena et al., 2006).

We found that *H1fnt* expression is significantly reduced in CKO RS compared with het RS controls, but is not changed in P/D cells in comparison with het P/D controls (Fig. 5F). This reduction in P/D-cell gene expression was confirmed by qRT-PCR with 21 dpp CKO and het control mouse testis extracts (Fig. S5C). The expression levels of the other known RS chromocenter formation-related genes we examined were not affected (Fig. 5F and Fig. S5C).

Taken together, these data suggest that the transition of a meiotic to a post-meiotic gene-expression program is impaired in *Ewsr1* CKO testes, and that this, in turn, leads to RS arrest and a block in spermiogenesis. In addition, the expression of some chromocenter formation-related genes is affected, which could explain the DNA condensation defects, which in turn prevent spermatid elongation.

Loss of EWSR1 does not affect chromatoid body integrity

Many of the genes with functions related to spermatid elongation and DNA condensation, including *Tnp2* and *Prm2*, are transcribed in spermatocytes and RS and stored in an RNA-protein complex termed the chromatoid body (Meikar et al., 2014; Peruquetti, 2015; Yokota, 2008). In chromatoid body-disrupted spermatids, in which the proper association between RNA-binding proteins and RNA cannot be retained, the mRNA content is altered by RNA degradation (Fanourgakis et al., 2016; Nagamori et al., 2011). To investigate whether the dysregulated mRNA levels we observed in *Ewsr1* CKO RS is due to disruption of the chromatoid body, we tested chromatin-body integrity by staining for MVH, an RNA helicase enriched in this structure. In both *Ewsr1* CKO and het controls, we observed a conspicuous perinuclear spot of MVH staining in RS, which suggested that the integrity of chromatoid bodies in the CKO was not affected (Fig. 6A). In addition, there was no significant difference between CKO and het control RS in expression of chromatoid body-related genes, including *Piwil1*, *Piwil2*, *Tdrd5*, *Tdrd6*, *Nsun* and *Mvh* (Fig. 6B), indicating that the major components of the chromatoid body are not affected by the absence of EWSR1. Our results strongly suggest that loss of EWSR1 in late pachytene spermatocytes leads to transcriptional changes but does not affect mRNA storage and processing.

DISCUSSION

In our previous work, using CKO mice lacking *Ewsr1* from the onset of meiosis, we showed that EWSR1 plays an essential role in meiotic recombination initiation (Tian et al., 2021). In the present study, using CKO mice lacking *Ewsr1* from the pachytene stage onward, we demonstrate that *Ewsr1* also acts as a regulator of spermiogenesis. Specifically, we show that EWSR1 is excluded from heterochromatin regions in pachytene/diplotene spermatocytes and round spermatids. Unlike the phenotype in CKO mice lacking *Ewsr1* from the onset of meiosis, deletion of *Ewsr1* from pachytene stage on does not affect any meiotic events, including chromosomal synapsis, DSB formation and crossover number. However, these CKO mice are sterile and lack elongated spermatids and mature sperm.

To identify the specific molecular mechanisms underlying the spermiogenesis defects caused by a lack of EWSR1, we performed RNA-seq with CKO pachytene spermatocytes and round spermatids, and, interestingly, determined that gene expression in CKO pachynema is not substantially altered, but that meiotic cell cycle-related genes are misregulated in round spermatids. Specifically, we showed that although high mRNA levels of the meiosis-specific proteins CNTD1, MLH1, L MOV10L1 and SYCP3 are retained in *Ewsr1* CKO RS, genes required for normal spermatid elongation and chromatin condensation, such *Prm1* and *Prm2*, genes that encode protamines (Cho et al., 2001), and *Tnp1* and *Tnp2*, which encode transition nuclear proteins (Shirley et al., 2004), are downregulated in

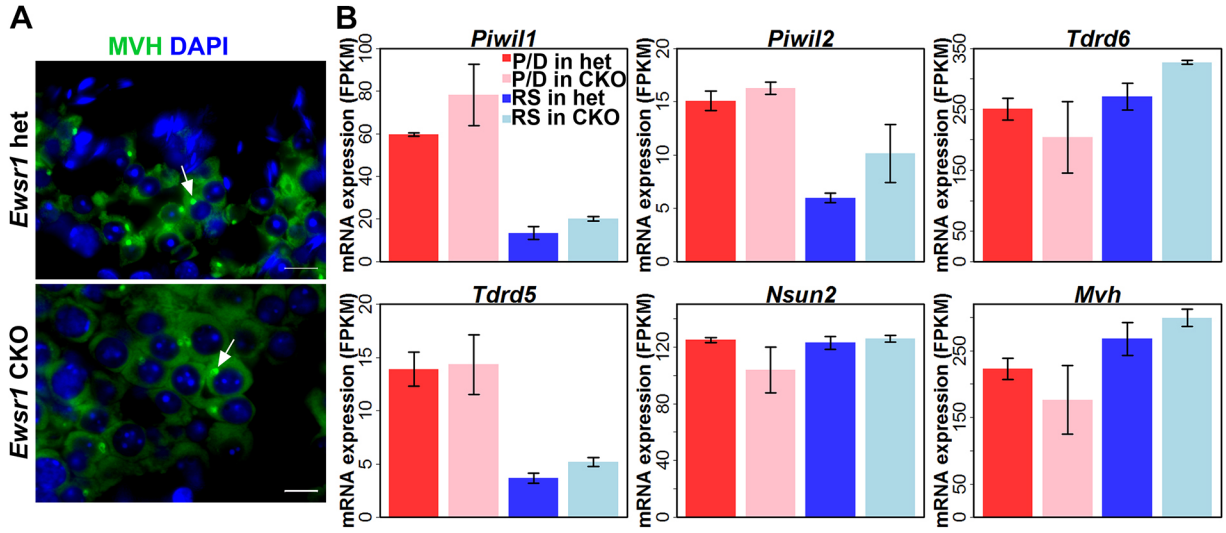

Fig. 6. Loss of EWSR1 does not affect chromatoid-body integrity. (A) Chromatoid bodies in *Ewsr1* het (top panel) and CKO (bottom panel) spermatids are labeled by anti-MVH antibody (green). Arrows indicate chromatoid bodies in RS. Scale bars: 10 µm. (B) mRNA level of chromatoid body formation, assessed via RNA-seq in het P/D cells (red), CKO P/D cells (pink), het RS (dark blue) and CKO RS (light blue). Data are mean±s.d.

Development (2021) 148, dev199414. doi:10.1242/dev.199414

CKO round spermatids. This misregulation most likely leads to DNA-packaging and chromatin-condensation defects in CKO spermatids.

In addition to meiotic cell cycle gene expression dysregulation, *Ewsr1* CKO round spermatids show severe chromocenter fragmentation. H1FNT (also known as HIST1T2 and H1T2) is a histone H1 variant specifically expressed in round and elongated spermatids. H1FNT is not required for acrosome formation per se (Martianov et al., 2005; Tanaka et al., 2005), but it associates with chromatin and is necessary for the polarity of nuclear chromatin organization and DNA condensation (Catena et al., 2006; Martianov et al., 2005; Tanaka et al., 2005). Therefore, reduction of *H1fnt* expression may affect the chromatin packaging required for spermatid elongation. The bipolar localization of H1FNT is regulated by TBPL1 and HMGB2 (Catena et al., 2006). *Tbpl1* and *Hmgb2* knockout mice both show chromocenter fragmentation defects, as well as disorganization of heterochromatin and dyslocalization of H1FNT (Catena et al., 2006; Martianov et al., 2002; Ronfani et al., 2001). BRDT is also known to be associated with spermiogenesis and chromocenter formation. The deletion of the first bromodomain of *Brdt* affects acetylated histone removal in elongating spermatids (Gaucher et al., 2012). This mutant also causes chromocenter fragmentation, depending on the genetic background (Berkovits and Wolgemuth, 2011), although this effect is dependent on the genetic background. However, expression of *Tbpl1*, *Hmgb2* and *Brdt* remains unaffected in pachytene spermatocytes or RS in the absence of EWSR1.

There are three possible explanations of how EWSR1 could be involved in regulating gene expression during spermiogenesis. First, EWSR1 may be involved in mRNA processing. Unlike in any other tissues, genes that are required for the final steps of spermatogenesis are transcribed in late meiotic cells and round spermatids, and their mRNAs are repressed and stored in a protein-RNA granule termed the chromatoid body (Braun, 1998). However, EWSR1 involvement in chromatoid body function is unlikely as the chromatoid-body integrity is not affected in *Ewsr1* CKO spermatids.

Second, EWSR1 may transcriptionally control the mRNA expression of the RS-upregulated genes. It is unlikely that EWSR1 regulates the altered gene expression directly, because our attempts to detect EWSR1 binding to DNA by EWSR1 ChIP-seq and affinity pull-down assays did not indicate that EWSR1 binds to DNA in germ cells on its own (data not shown). However, EWSR1 is reported to bind to and modulate the functions of other RNA-binding proteins and transcriptional factors (Bertolotti et al., 1998; Petermann et al., 1998; Yang et al., 2000). In this regard, it remains possible that EWSR1 mediates gene transcription as a component of complexes involving those RNA-binding proteins and transcriptional factors.

Third, EWSR1 has been shown to be broadly involved in primary miRNA processing (He and Ding, 2020; Kim et al., 2015; Ouyang et al., 2017), raising the possibility that, in the absence of EWSR1, many downstream genes may be affected by aberrant post-transcriptional control resulting from dysregulation of miRNAs. With our current data, we cannot confirm or rule out either of the second or third possibility.

In summary, our results show that EWSR1 has two completely different functions in germ cell development – one in recombination regulation (Tian et al., 2021) and another in spermatid development (this article). These functions are related to the distinct expression pattern of EWSR1 – low expression in early meiosis, and dramatic increase at and after the pachytene stage. The latter function of EWSR1 is more reminiscent of those of the TET family proteins in somatic cells (Tan and Manley, 2009). Together, our data emphasize the nature of EWSR1 as a multifunctional protein. Further research characterizing the functions of its individual domains in different cell types would be necessary to elucidate the mechanisms of its multifunctionality.

MATERIALS AND METHODS

Ethics statement

The animal care rules used by The Jackson Laboratory are compatible with the regulations and standards of the US Department of Agriculture and the National Institutes of Health. The protocols used in this study were approved by the Animal Care and Use Committee of The Jackson Laboratory (Summary #04008). Euthanasia for this study was carried out by cervical dislocation.

Mating scheme for generation of Ewsr1 CKO mice

Information on the sources of the strains used to generate the *Ewsr1* CKO mice used in this study is provided in the section 'Mouse strains used in this project'. The *Ewsr1* CKO mice used in this study were produced by a two-step deletion scheme. C57BL/6N-Ewsr1$^{<tm1c(EUCOMM)Wtsi>}$/Tcp mice were mated to Tg(Sox2-cre)1Amc/J mice to generate one *Ewsr1* allele deleted mice, and then the *Ewsr1* hemizygous mice (*Ewsr1*$^{\Delta/+}$) were mated to C57BL/6-Tg(Hspa2-cre)1Eddy/J to obtain *Ewsr1*$^{\Delta/+;Hspa\text{-}Cre}$ mice. The *Ewsr1*$^{\Delta/+;Hspa\text{-}Cre}$ mice were mated to homozygous *Ewsr1* loxp mice to generate heterozygous control mice (*Ewsr1*$^{loxp/+;Hspa\text{-}Cre}$, *Ewsr1* het) or conditional knockout mice (*Ewsr1*$^{loxp/\Delta;Hspa\text{-}Cre}$, *Ewsr1* CKO).

Mouse strains used in this project

The mouse line C57BL/6N-Ewsr1$^{<tm1c(EUCOMM)Wtsi>}$/Tcp was made as part of the NorCOMM2 project at the Toronto Centre for Phenogenomics (Bradley et al., 2012) and obtained from the Canadian Mouse Mutant Repository. C57BL/6J (stock number 000664), Tg(Sox2-cre)1Amc/J (stock number 004783) and C57BL/6-Tg(Hspa2-cre)1Eddy/J (stock number 008870) mice were obtained from The Jackson Laboratory. All animal experiments were approved by the Animal Care and Use Committee of The Jackson Laboratory (Summary #04008).

Histology and immunostaining

For histological evaluation, testis or epididymis were dissected out, fixed with Bouin's solution and embedded in paraffin wax, and 5 µm sections were prepared. Sections were stained with Hematoxylin and Eosin or periodic acid-Schiff-diastase (PAS) using standard techniques.

For preparation of nuclear spreads from germ cells, the drying-down technique (Peters et al., 1997) was used, followed by immunolabeling with anti-SYCP3 (NB300-231, Novus Biologicals, 1:500), anti-γH2AX (ab26350, Abcam, 1:1000), anti-ATR (sc-1887, Santa Cruz, 1:500), anti-HORMAD1 (13917-1-AP, Protein Tech, 1:500), anti-MLH1 (550838, BD Pharmingen, 1:100) or anti-centromere (CREST) (15-234-0001, Antibodies Incorporated, 1:50) antibodies.

FACS and RNA-sequencing

FACS was essentially carried out according to Lam et al. (2019). Adult testes from *Ewsr1* het and CKO mice were placed in 10 ml EKRB [1×KRB with 100 nM $CaCl_2$, 200 mmM L-Glutamine-Penicillin-Streptomycin solution, 1× MEM essential amino acids, 1× MEM non-essential amino acids, 0.05 mg/ml lactate sodium, 0.72 mg/ml sodium pyruvate and 20 mM HEPES buffer (pH 7.25)] with 0.5 mg/ml collagenase IV and 0.5 µg/ml DnaseI, and incubated in a shaker at 32°C for 20 min at 120 rpm. After incubation, seminiferous tubules were pipetted 20 times with a 10 ml pipette for, and spun down at 800 rpm (300 ***g***) for 10 min. The supernatant was then removed and tubules were washed with 10 ml EKRB with 0.5 mg/ml collagenase IV and 0.5 µg/ml DnaseI, and incubated in a shaker at 32°C for 20 min at 120 rpm. After pipetting again 20 times, tubules were filtered with a 40 µm mesh, spun down at 1000 rpm (400 ***g***) for 10 min, and then washed three times with 20 ml EKRB . The cells were resuspended in 1 ml EKRB containing 1% FBS, filtered with a 40 µm mesh and diluted to 6000 cells/µl with 1% FBS/EKRB. The cells were then stained with 5 µl/ml Hoechst

Development (2021) 148, dev199414. doi:10.1242/dev.199414

33342 (ThermoFisher, H1399) and 0.5 µl/ml DnaseI in the dark at 32°C. Before loading the cell for sorting, 2 µl/ml propidium iodide was added to samples. Then, 0.5 million 4c pachynema and 1 million 2c round spermatids were sorted into EKRB with 1% FBS, after which the RNA was isolated by a standard method and RNA-seq libraries are prepared with a KAPA RNA Hyper Prep Kit (KAPABIOSYSTEM, KK8540).

Libraries were sequenced on an Illumina HiSeq 2500, with 75 bp paired-end reads. Fastq files for paired-end sequenced DMC1 samples were trimmed using Trimmomatic (v0.32) (Bolger et al., 2014). The trimmed fastq files were aligned to mouse genome mm10 using Bowtie (2.2.0) (Langmead and Salzberg, 2012). The software package RSEM (1.2.12) (Li and Dewey, 2011) was then used for gene annotation, calculation of fragments per kilobase million (FPKM) and normalization. For each cell group (*Ewrs1* het P/D and RS samples, *Ewsr1* CKO P/D and RS samples), the correlations among the replicates are high (r2=0.99 for Ewsr1 het P/D and RS samples, and *Ewsr1* CKO RS samples; r^2=0.96 for *Ewsr1* CKO P/D samples). Differentially expressed genes were analyzed using Gene Ontology Enrichment Analysis (http://www.geneontology.org/page/go-enrichment-analysis).

RNA isolation and quantitative PCR (qPCR)

Total RNA from 21 dpp *Ewsr1* het and CKO mouse testes was isolated with a mirVana miRNA isolation kit (AM1560, Applied Biosystems). qPCR was performed with Quantifast SYBR Green PCR kit (204054, Qiagen). β-Actin mRNA levels were used for normalization. Primer sequences for qPCR were: β-actin forward, TGGCTCCTAGCACCATGAA; β-actin reverse, CTCAGTAACAGTCCGCCTAGAAGCA; *Brdt* forward, GGTCCAAAT-TACAAAGGGTGTGAAG; *Brdt* reverse, GTCGGAGGAGATTCGCTA-CTTG; *Tbpl1* forward, TCTGGCAAGCTGGTCTCTGT; *Tbpl1* reverse, CCTCCAGTCACCCTTCACAT; *Hmgb2* forward, GGCCAGCCTGTC-TACAGAG; *Hmgb2* reverse, GTTGGGTAGGCTGCTATCAAGA; *H1fnt* forward, CCAGTAAAACAGACCATCCAGA; and *H1fnt* reverse, CTGGCATTAAGGAGACTCAGTG.

Acknowledgements

We thank Tim Billings for technical help and Mary Ann Handel for critical reading of the manuscript. This article is dedicated to the memory of Ken Paigen, an excellent colleague, mentor and visionary.

Competing interests

The authors declare no competing or financial interests.

Author contributions

Conceptualization: H.T., P.M.P.; Methodology: H.T.; Validation: H.T.; Formal analysis: H.T., P.M.P.; Investigation: H.T.; Resources: P.M.P.; Writing - original draft: H.T.; Writing - review & editing: P.M.P.; Supervision: P.M.P.; Project administration: P.M.P.; Funding acquisition: P.M.P.

Funding

This work was supported by National Institutes of Health (R01 GM078452 to P.M.P., P50 GM076468 to Gary Churchill/Project B to P.M.P.) and by a Cancer Core Grant (National Cancer Institute; CA34196M to the Jackson Laboratory). Deposited in PMC for release after 12 months.

Data availability

The RNA-seq data have been deposited in GEO under accession number GSE120989.

Peer review history

The peer review history is available online at https://journals.biologists.com/dev/article-lookup/doi/10.1242/dev.199414

References

Barral, S., Morozumi, Y., Tanaka, H., Montellier, E., Govin, J., de Dieuleveult, M., Charbonnier, G., Coute, Y., Puthier, D., Buchou, T. et al. (2017). Histone variant H2A.L.2 guides transition protein-dependent protamine assembly in male germ cells. *Mol. Cell* **66**, 89-101.e108. doi:10.1016/j.molcel.2017.02.025

Berkovits, B. D. and Wolgemuth, D. J. (2011). The first bromodomain of the testis-specific double bromodomain protein Brdt is required for chromocenter organization that is modulated by genetic background. *Dev. Biol.* **360**, 358-368. doi:10.1016/j.ydbio.2011.10.005

Berkovits, B. D. and Wolgemuth, D. J. (2013). The role of the double bromodomain-containing BET genes during mammalian spermatogenesis. *Curr. Top. Dev. Biol.* **102**, 293-326. doi:10.1016/B978-0-12-416024-8.00011-8

Bertolotti, A., Melot, T., Acker, J., Vigneron, M., Delattre, O. and Tora, L. (1998). EWS, but not EWS-FLI-1, is associated with both TFIID and RNA polymerase II: interactions between two members of the TET family, EWS and hTAFII68, and subunits of TFIID and RNA polymerase II complexes. *Mol. Cell. Biol.* **18**, 1489-1497. doi:10.1128/MCB.18.3.1489

Bolger, A. M., Lohse, M. and Usadel, B. (2014). Trimmomatic: a flexible trimmer for Illumina sequence data. *Bioinformatics* **30**, 2114-2120. doi:10.1093/bioinformatics/btu170

Bradley, A., Anastassiadis, K., Ayadi, A., Battey, J. F., Bell, C., Birling, M. C., Bottomley, J., Brown, S. D., Burger, A., Bult, C. J. et al. (2012). The mammalian gene function resource: the international knockout mouse consortium. *Mamm. Genome* **23**, 580-586. doi:10.1007/s00335-012-9422-2

Braun, R. E. (1998). Post-transcriptional control of gene expression during spermatogenesis. *Semin. Cell Dev. Biol.* **9**, 483-489. doi:10.1006/scdb.1998.0226

Brinkley, B. R., Brenner, S. L., Hall, J. M., Tousson, A., Balczon, R. D. and Valdivia, M. M. (1986). Arrangements of kinetochores in mouse cells during meiosis and spermiogenesis. *Chromosoma* **94**, 309-317. doi:10.1007/BF00290861

Catena, R., Ronfani, L., Sassone-Corsi, P. and Davidson, I. (2006). Changes in intranuclear chromatin architecture induce bipolar nuclear localization of histone variant H1T2 in male haploid spermatids. *Dev. Biol.* **296**, 231-238. doi:10.1016/j.ydbio.2006.04.458

Chansky, H. A., Hu, M., Hickstein, D. D. and Yang, L. (2001). Oncogenic TLS/ERG and EWS/Fli-1 fusion proteins inhibit RNA splicing mediated by YB-1 protein. *Cancer Res.* **61**, 3586-3590.

Cho, C., Willis, W. D., Goulding, E. H., Jung-Ha, H., Choi, Y. C., Hecht, N. B. and Eddy, E. M. (2001). Haploinsufficiency of protamine-1 or -2 causes infertility in mice. *Nat. Genet.* **28**, 82-86. doi:10.1038/ng0501-82

Delattre, O., Zucman, J., Plougastel, B., Desmaze, C., Melot, T., Peter, M., Kovar, H., Joubert, I., de Jong, P., Rouleau, G. et al. (1992). Gene fusion with an ETS DNA-binding domain caused by chromosome translocation in human tumours. *Nature* **359**, 162-165. doi:10.1038/359162a0

de Mateo, S. and Sassone-Corsi, P. (2014). Regulation of spermatogenesis by small non-coding RNAs: role of the germ granule. *Semin. Cell Dev. Biol.* **29**, 84-92. doi:10.1016/j.semcdb.2014.04.021

Fanourgakis, G., Lesche, M., Akpinar, M., Dahl, A. and Jessberger, R. (2016). Chromatoid body protein TDRD6 supports long 3′ UTR triggered nonsense mediated mRNA decay. *PLoS Genet.* **12**, e1005857. doi:10.1371/journal.pgen.1005857

Frost, R. J., Hamra, F. K., Richardson, J. A., Qi, X., Bassel-Duby, R. and Olson, E. N. (2010). MOV10L1 is necessary for protection of spermatocytes against retrotransposons by Piwi-interacting RNAs. *Proc. Natl. Acad. Sci. USA* **107**, 11847-11852. doi:10.1073/pnas.1007158107

Fujii, Y., Fujita, H. and Yokota, S. (2017). Synthesis of beta-tubulin occurs within chromatoid body of round spermatids. *Cytoskeleton* **74**, 197-204. doi:10.1002/cm.21363

Gaucher, J., Boussouar, F., Montellier, E., Curtet, S., Buchou, T., Bertrand, S., Hery, P., Jounier, S., Depaux, A., Vitte, A. L. et al. (2012). Bromodomain-dependent stage-specific male genome programming by Brdt. *EMBO J.* **31**, 3809-3820. doi:10.1038/emboj.2012.233

He, P. and Ding, J. (2020). EWS promotes cell proliferation and inhibits cell apoptosis by regulating miR-199a-5p/Sox2 axis in osteosarcoma. *Biotechnol. Lett.* **42**, 1263-1274. doi:10.1007/s10529-020-02859-4

Hess, R. A. and Renato de Franca, L. (2008). Spermatogenesis and cycle of the seminiferous epithelium. *Adv. Exp. Med. Biol.* **636**, 1-15. doi:10.1007/978-0-387-09597-4_1

Holloway, J. K., Sun, X. F., Yokoo, R., Villeneuve, A. M. and Cohen, P. E. (2014). Mammalian CNTD1 is critical for meiotic crossover maturation and deselection of excess precrossover sites. *J. Cell Biol.* **205**, 633-641. doi:10.1083/jcb.201401122

Hoyer-Fender, S., Singh, P. B. and Motzkus, D. (2000). The murine heterochromatin protein M31 is associated with the chromocenter in round spermatids and Is a component of mature spermatozoa. *Exp. Cell Res.* **254**, 72-79. doi:10.1006/excr.1999.4729

Idler, R. K. and Yan, W. (2012). Control of messenger RNA fate by RNA-binding proteins: an emphasis on mammalian spermatogenesis. *J. Androl.* **33**, 309-337. doi:10.2164/jandrol.111.014167

Inselman, A. L., Nakamura, N., Brown, P. R., Willis, W. D., Goulding, E. H. and Eddy, E. M. (2010). Heat shock protein 2 promoter drives Cre expression in spermatocytes of transgenic mice. *Genesis* **48**, 114-120. doi:10.1002/dvg.20588

Kim, K. Y., Hwang, Y. J., Jung, M. K., Choe, J., Kim, Y., Kim, S., Lee, C. J., Ahn, H., Lee, J., Kowall, N. W. et al. (2014). A multifunctional protein EWS regulates the expression of Drosha and microRNAs. *Cell Death Differ.* **21**, 136-145. doi:10.1038/cdd.2013.144

Kim, Y., Kang, Y.-S., Lee, N.-Y., Kim, K. Y., Hwang, Y. J., Kim, H.-W., Rhyu, I. J., Her, S., Jung, M.-K., Kim, S. et al. (2015). Uvrag targeting by Mir125a and Mir351

modulates autophagy associated with Ewsr1 deficiency. *Autophagy* **11**, 796-811. doi:10.1080/15548627.2015.1035503

Knoop, L. L. and Baker, S. J. (2000). The splicing factor U1C represses EWS/FLI-mediated transactivation. *J. Biol. Chem.* **275**, 24865-24871. doi:10.1074/jbc.M001661200

Lam, K.-G., Brick, K., Cheng, G., Pratto, F. and Camerini-Otero, R. D. (2019). Cell-type-specific genomics reveals histone modification dynamics in mammalian meiosis. *Nat. Commun.* **10**, 3821. doi:10.1038/s41467-019-11820-7

Langmead, B. and Salzberg, S. L. (2012). Fast gapped-read alignment with Bowtie 2. *Nat. Methods* **9**, U357-U354. doi:10.1038/nmeth.1923

Lehti, M. S. and Sironen, A. (2016). Formation and function of the manchette and flagellum during spermatogenesis. *Reproduction* **151**, R43-R54. doi:10.1530/REP-15-0310

Li, B. and Dewey, C. N. (2011). RSEM: accurate transcript quantification from RNA-Seq data with or without a reference genome. *BMC Bioinformatics* **12**, 323. doi:10.1186/1471-2105-12-323

Li, H., Watford, W., Li, C., Parmelee, A., Bryant, M. A., Deng, C., O'Shea, J. and Lee, S. B. (2007). Ewing sarcoma gene EWS is essential for meiosis and B lymphocyte development. *J. Clin. Invest.* **117**, 1314-1323. doi:10.1172/JCI31222

Margolin, G., Khil, P. P., Kim, J., Bellani, M. A. and Camerini-Otero, R. D. (2014). Integrated transcriptome analysis of mouse spermatogenesis. *BMC Genomics* **15**, 39. doi:10.1186/1471-2164-15-39

Martianov, I., Brancorsini, S., Gansmuller, A., Parvinen, M., Davidson, I. and Sassone-Corsi, P. (2002). Distinct functions of TBP and TLF/TRF2 during spermatogenesis: requirement of TLF for heterochromatic chromocenter formation in haploid round spermatids. *Development* **129**, 945-955. doi:10.1242/dev.129.4.945

Martianov, I., Brancorsini, S., Catena, R., Gansmuller, A., Kotaja, N., Parvinen, M., Sassone-Corsi, P. and Davidson, I. (2005). Polar nuclear localization of H1T2, a histone H1 variant, required for spermatid elongation and DNA condensation during spermiogenesis. *Proc. Natl. Acad. Sci. USA* **102**, 2808-2813. doi:10.1073/pnas.0406060102

Meikar, O., Da Ros, M., Korhonen, H. and Kotaja, N. (2011). Chromatoid body and small RNAs in male germ cells. *Reproduction* **142**, 195-209. doi:10.1530/REP-11-0057

Meikar, O., Vagin, V. V., Chalmel, F., Sostar, K., Lardenois, A., Hammell, M., Jin, Y., Da Ros, M., Wasik, K. A., Toppari, J. et al. (2014). An atlas of chromatoid body components. *RNA* **20**, 483-495. doi:10.1261/rna.043729.113

Nagamori, I., Cruickshank, V. A. and Sassone-Corsi, P. (2011). Regulation of an RNA granule during spermatogenesis: acetylation of MVH in the chromatoid body of germ cells. *J. Cell Sci.* **124**, 4346-4355. doi:10.1242/jcs.096461

Namekawa, S. H., Park, P. J., Zhang, L.-F., Shima, J. E., McCarrey, J. R., Griswold, M. D. and Lee, J. T. (2006). Postmeiotic sex chromatin in the male germline of mice. *Curr. Biol.* **16**, 660-667. doi:10.1016/j.cub.2006.01.066

Nantel, F., Monaco, L., Foulkes, N. S., Masquilier, D., LeMeur, M., Henriksen, K., Dierich, A., Parvinen, M. and Sassone-Corsi, P. (1996). Spermiogenesis deficiency and germ-cell apoptosis in CREM-mutant mice. *Nature* **380**, 159-162. doi:10.1038/380159a0

Ouyang, H. W., Zhang, K., Fox-Walsh, K., Yang, Y., Zhang, C., Huang, J., Li, H., Zhou, Y. and Fu, X. D. (2017). The RNA binding protein EWS is broadly involved in the regulation of pri-miRNA processing in mammalian cells. *Nucleic Acids Res.* **45**, 12481-12495. doi:10.1093/nar/gkx912

Paronetto, M. P. and Sette, C. (2010). Role of RNA-binding proteins in mammalian spermatogenesis. *Int. J. Androl.* **33**, 2-12. doi:10.1111/j.1365-2605.2009.00959.x

Paronetto, M. P., Minana, B. and Valcarcel, J. (2011). The Ewing sarcoma protein regulates DNA damage-induced alternative splicing. *Mol. Cell* **43**, 353-368. doi:10.1016/j.molcel.2011.05.035

Parvanov, E. D., Tian, H., Billings, T., Saxl, R. L., Spruce, C., Aithal, R., Krejci, L., Paigen, K. and Petkov, P. M. (2017). PRDM9 interactions with other proteins provide a link between recombination hotspots and the chromosomal axis in meiosis. *Mol. Biol. Cell* **28**, 488-499. doi:10.1091/mbc.e16-09-0686

Peruquetti, R. L. (2015). Perspectives on mammalian chromatoid body research. *Anim. Reprod. Sci.* **159**, 8-16. doi:10.1016/j.anireprosci.2015.05.018

Petermann, R., Mossier, B. M., Aryee, D. N., Khazak, V., Golemis, E. A. and Kovar, H. (1998). Oncogenic EWS-Fli1 interacts with hsRPB7, a subunit of human RNA polymerase II. *Oncogene* **17**, 603-610. doi:10.1038/sj.onc.1201964

Peters, A. H., Plug, A. W., van Vugt, M. J. and de Boer, P. (1997). A drying-down technique for the spreading of mammalian meiocytes from the male and female germline. *Chromosome Res.* **5**, 66-68. doi:10.1023/A:1018445520117

Rathke, C., Baarends, W. M., Awe, S. and Renkawitz-Pohl, R. (2014). Chromatin dynamics during spermiogenesis. *Biochim. Biophys. Acta* **1839**, 155-168. doi:10.1016/j.bbagrm.2013.08.004

Ronfani, L., Ferraguti, M., Croci, L., Ovitt, C. E., Scholer, H. R., Consalez, G. G. and Bianchi, M. E. (2001). Reduced fertility and spermatogenesis defects in mice lacking chromosomal protein Hmgb2. *Development* **128**, 1265-1273. doi:10.1242/dev.128.8.1265

Santucci-Darmanin, S., Walpita, D., Lespinasse, F., Desnuelle, C., Ashley, T. and Paquis-Flucklinger, V. (2000). MSH4 acts in conjunction with MLH1 during mammalian meiosis. *FASEB J.* **14**, 1539-1547. doi:10.1096/fj.99-0851com

Schmid, R., Grellscheid, S. N., Ehrmann, I., Dalgliesh, C., Danilenko, M., Paronetto, M. P., Pedrotti, S., Grellscheid, D., Dixon, R. J., Sette, C. et al. (2013). The splicing landscape is globally reprogrammed during male meiosis. *Nucleic Acids Res.* **41**, 10170-10184. doi:10.1093/nar/gkt811

Schwartz, J. C., Cech, T. R. and Parker, R. R. (2015). Biochemical Properties and Biological Functions of FET Proteins. *Annu. Rev. Biochem.* **84**, 355-379. doi:10.1146/annurev-biochem-060614-034325

Shirley, C. R., Hayashi, S., Mounsey, S., Yanagimachi, R. and Meistrich, M. L. (2004). Abnormalities and reduced reproductive potential of sperm from Tnp1- and Tnp2-null double mutant mice. *Biol. Reprod.* **71**, 1220-1229. doi:10.1095/biolreprod.104.029363

Steger, K. (1999). Transcriptional and translational regulation of gene expression in haploid spermatids. *Anat. Embryol.* **199**, 471-487. doi:10.1007/s004290050245

Tan, A. Y. and Manley, J. L. (2009). The TET family of proteins: functions and roles in disease. *J. Mol. Cell Biol.* **1**, 82-92. doi:10.1093/jmcb/mjp025

Tanaka, H., Iguchi, N., Isotani, A., Kitamura, K., Toyama, Y., Matsuoka, Y., Onishi, M., Masai, K., Maekawa, M., Toshimori, K. et al. (2005). HANP1/H1T2, a novel histone H1-like protein involved in nuclear formation and sperm fertility. *Mol. Cell. Biol.* **25**, 7107-7119. doi:10.1128/MCB.25.16.7107-7119.2005

Tian, H., Billings, T. and Petkov, P. M. (2021). EWSR1 affects PRDM9-dependent histone 3 methylation and provides a link between recombination hotspots and the chromosome axis protein REC8. *Mol. Biol. Cell* **32**, 1-14. doi:10.1091/mbc.E20-09-0604

Visser, L. and Repping, S. (2010). Unravelling the genetics of spermatogenic failure. *Reproduction* **139**, 303-307. doi:10.1530/REP-09-0229

Vourekas, A., Zheng, K., Fu, Q., Maragkakis, M., Alexiou, P., Ma, J., Pillai, R. S., Mourelatos, Z. and Wang, P. J. (2015). The RNA helicase MOV10L1 binds piRNA precursors to initiate piRNA processing. *Genes Dev.* **29**, 617-629. doi:10.1101/gad.254631.114

Yang, L., Chansky, H. A. and Hickstein, D. D. (2000). EWS.Fli-1 fusion protein interacts with hyperphosphorylated RNA polymerase II and interferes with serine-arginine protein-mediated RNA splicing. *J. Biol. Chem.* **275**, 37612-37618. doi:10.1074/jbc.M005739200

Yokota, S. (2008). Historical survey on chromatoid body research. *Acta Histochem. Cytochem.* **41**, 65-82. doi:10.1267/ahc.08010

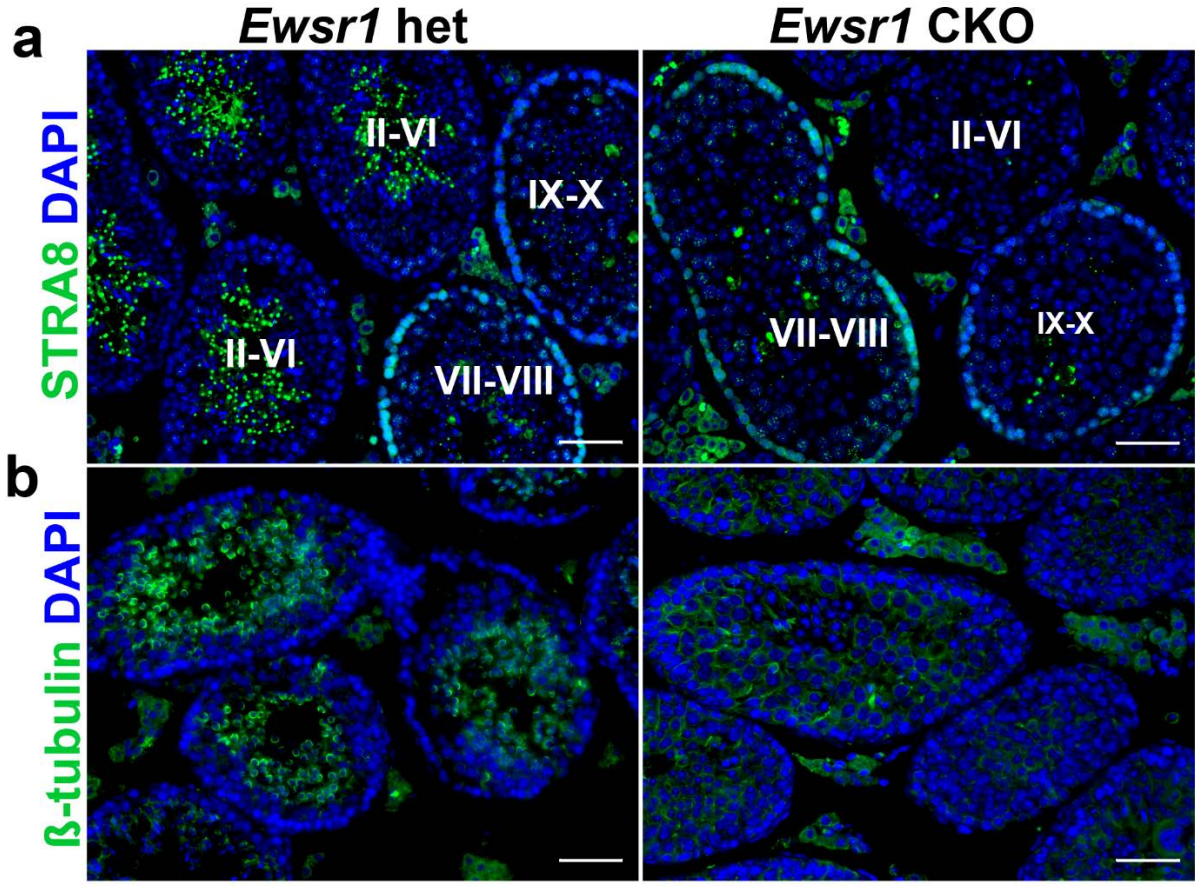

Figure S1. Loss of elongated spermatids in *Ewsr1* CKO seminiferous tubules.

(A) Immunostaining of STRA8 (green) in *Ewsr1* het (left panel) and CKO (right panel) testicular cross sections. The numbers indicate the stage of each seminiferous tubule. (B) Immunostaining of the elongated spermatid marker ß-tubulin in *Ewsr1* het (left panel) and CKO (right panel) testicular cross sections. Scale bar, 50 µm.

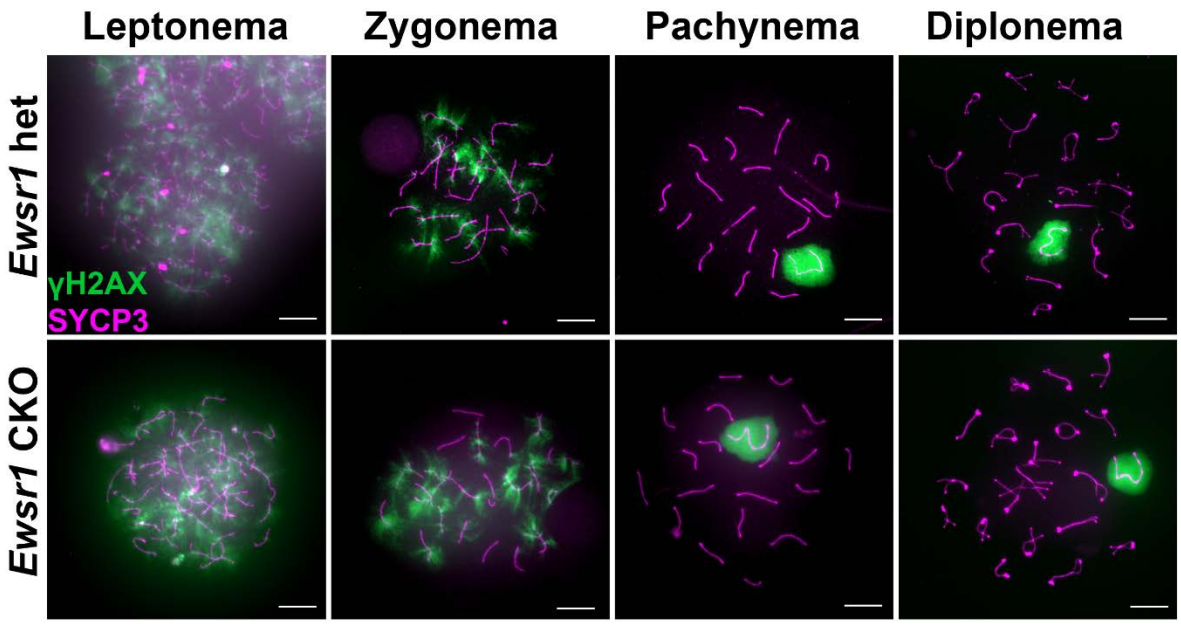

Figure S2. Meiotic recombination is not affected in the absence of EWSR1.

Immunostaining of γH2AX (green) and SYCP3 (magenta) in leptonema, zygonema, pachynema and diplonema of *Ewsr1* het (top panels) and CKO (bottom panels) spermatocytes.

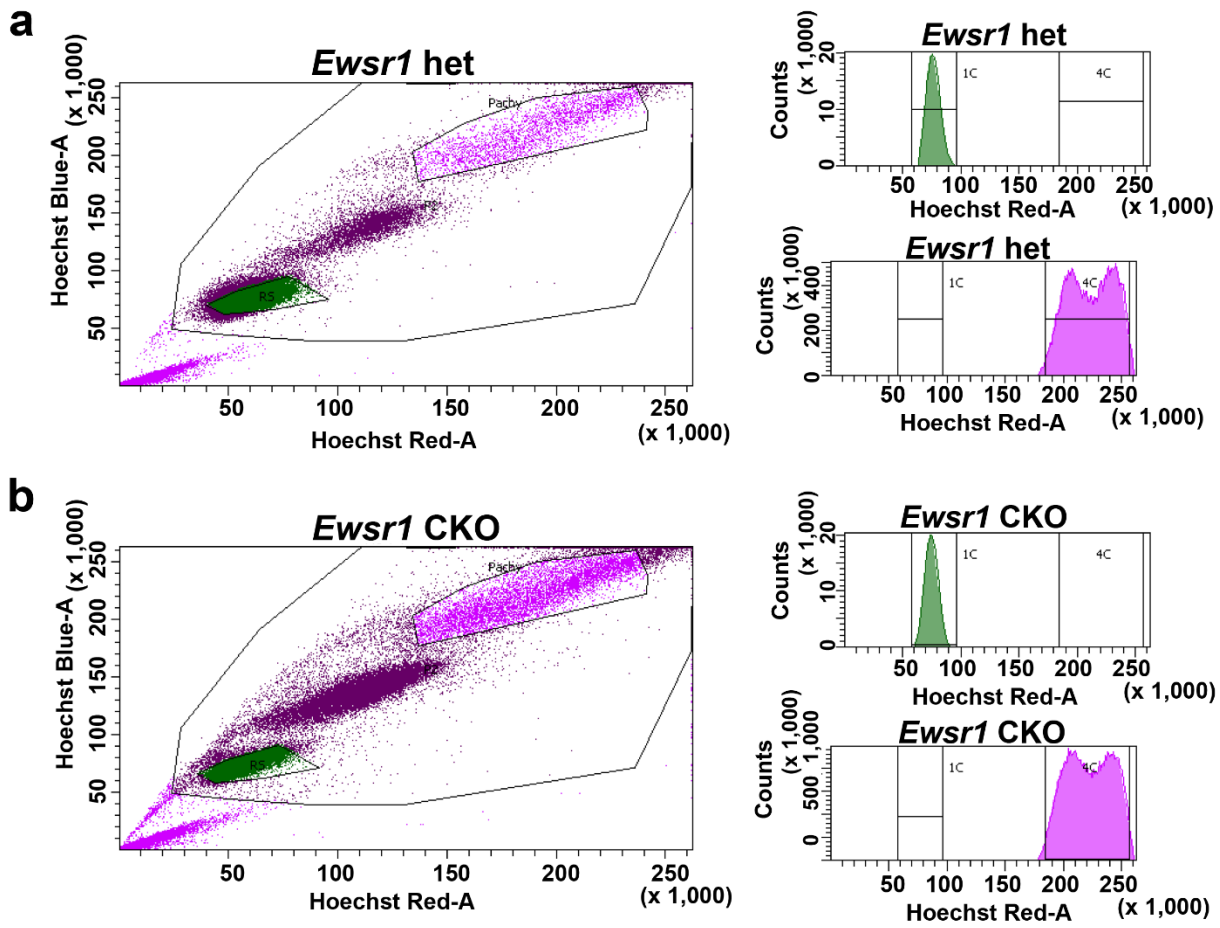

Figure S3. Flow cytometry sorting of pachynema/diplonema and round spermatids in *Ewsr1* het and CKO mice.

(A and B) 4C (pachynema/diplonema) and 1C (RS) cells were sorted based on DNA content by Hoechst 43342 staining of *Ewsr1* het (A) and CKO (B) isolated testicular germ cells.

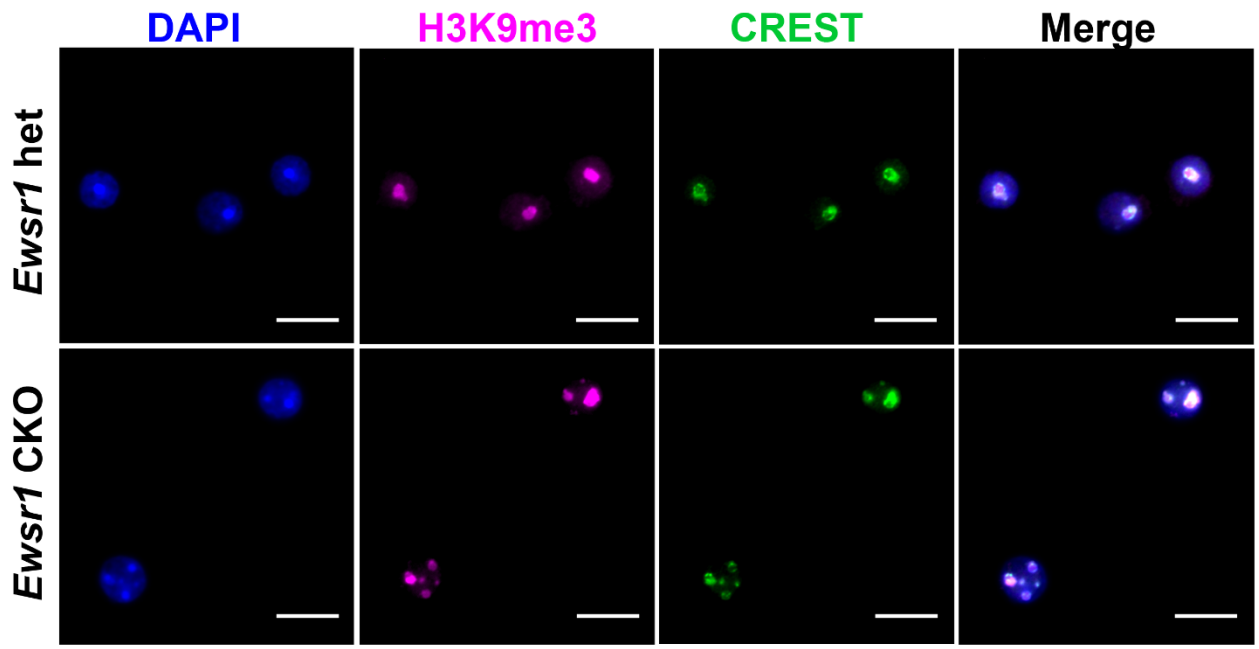

Figure S4. Increased chromocenter fragmentation in isolated round spermatids in *Ewsr1* CKO mice.

Co-immunostaining of H3K9me3 (magenta) and centromeres (CREST, green) in flow cytometry-sorted RS in *Ewsr1* het (top panels) and CKO (bottom panels) mice. Scale bar, 10 µm.

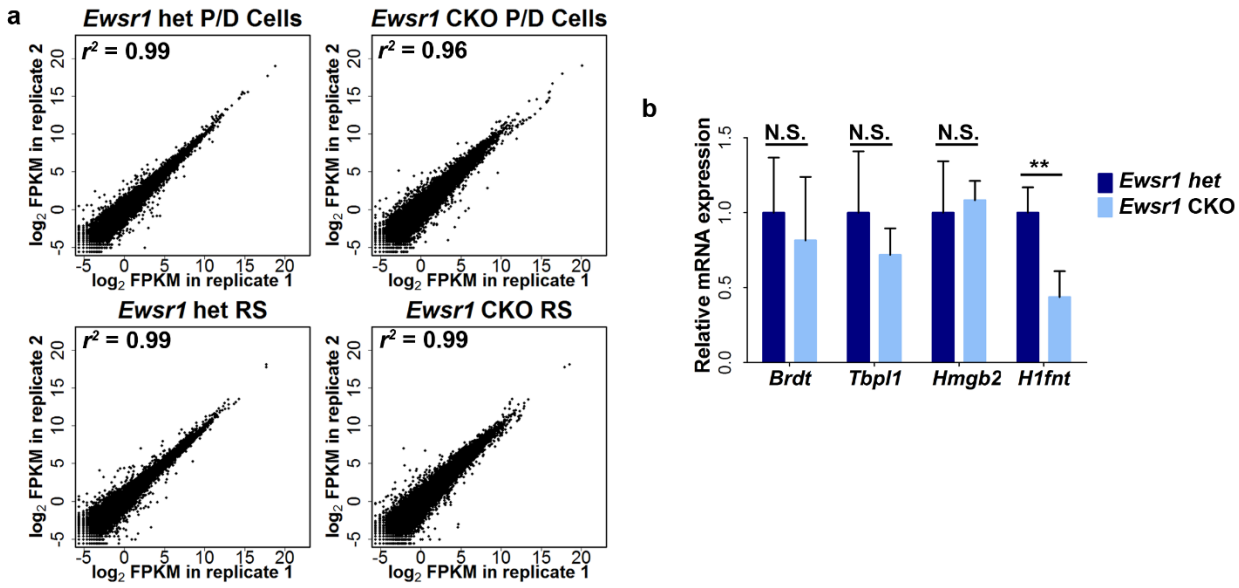

Figure S5. The transition from a meiotic to a spermiogenesis gene-expression program is affected in *Ewsr1* CKO mice.

(A) Correlation between replicates of P/D and of RS samples. R^2 values are shown in the upper left-hand corners. (B) QRT-PCR of chromocenter formation-related genes expression in 21-dpp *Ewsr1* het (dark blue) and CKO (light blue) mouse testis extracts. *β-Actin* mRNA levels were used for normalization. N.S., not significant ($p > 0.05$ by Student's *t*-test), ** $p < 0.01$ by Student's *t*-test. Data is shown as mean ± SD with 3 replicates.